Emergent Geometry From Hamiltonian-space Renormalization Group in Many-body Localized Systems

Tamra Nebabu
Department of Physics, Stanford University, Stanford, CA 94305
(Dated: January 7, 2021)

Submitted as coursework for PH470, Stanford University, Spring 2020

We review recent renormalization group (RG) methods for studying the transition between the many-body localized (MBL) and thermalized phases. Conventional real-space RG protocols involve coarse-graining the degrees of freedom into thermal and insulating blocks, and calculating critical exponents from (FILL IN). A more recent approach defines an RG flow in Hamiltonian space in order to find the emergent local integrals of motion in the MBL phase. One advantage of this approach is that it can potentially be used to study MBL in an arbitrary number of dimensions. On can understand the Hamiltonian-space flow as being performed by a tensor network, and the holographic interpretation of the flow leads to a fragmented network geometry.

I. INTRODUCTION

A. The MBL and ETH phases

According to the eigenstate thermalization hypothesis (ETH), a large class of isolated quantum many-body systems are capable of reaching thermal equilibrium. This means that the expectation values of few-body observables at late times are well predicted by the energy of the system rather than by the microscopic degrees of freedom, just as in the classical Gibbs ensemble[4,18]. One can understand thermalization as resulting from the isolated system acting as a thermal bath for itself. Under unitary time evolution, information about the system's initial conditions is scrambled among nonlocal degrees of freedom, making such information inaccessible to few-body operators[5]. The ETH postulates an explanation for this scrambling that relies on the random-vector properties of individual energy eigenstates in a non-integrable system[4,11]. In the thermodynamic limit, the large entanglement entropy of any finite subsystem will cause its reduced density matrix to converge to the equilibrium thermal distribution[13].

However, there is a notable exception to the ETH: in the presence of a strongly-disordered potential, non-integrable systems can fail to thermalize—a phenomenon known as many-body localization (MBL). In an MBL system, disorder generates energetic detuning between eigenstates with similar microscopic configurations. Hence, the expectation values of local observables are no longer a smooth function of energy in the thermodynamic limit and therefore do not follow the microcanonical ensemble. The presence of disorder in localized systems dramatically slows the spread of quantum information, leading to a failure to come to equilibrium[5]. The eigenstates are said to be "localized," i.e. exhibit subthermal "area-law" entanglement entropy, analogous to the ground states of local Hamiltonians. The novelty of MBL systems comes from the fact that these features can persist for highly-excited eigenstates at large energy densities.

One can understand localization and thermalization as different phases of the same disordered Hamiltonian. A canonical example in 1D is the following Hamiltonian[9,10] written in terms of spin degrees of freedom:

$$H = \sum_i h_i s_i^z + J \sum_i \boldsymbol{S}_i \cdot \boldsymbol{S}_{i+1} + \dots \tag{1}$$

where $\boldsymbol{S}_i$ represents the total spin vector for the i^{th} spin $\boldsymbol{S}_i = (s_i^x, s_i^y, s_i^z)$ and h_i is a random field drawn from the uniform distribution $[-W, W]$. The ellipsis indicates the possibility of including progressively less-local interactions, such next-nearest neighbor interactions.

In the absence of interactions, the Hamiltonian is integrable and possesses an extensive number of conserved quantities, or local integrals of motion (LIOMs). Furthermore, the eigenstates are localized and randomly distributed in energy space[i]. In the strong disorder regime ($W >> J$) one can treat the interaction terms perturbatively, and the eigenstates will mostly retain their local character. This is because the matrix elements of the interaction only significantly couple eigenstates with similar configurations and one must go to higher-orders in perturbation theory to hybridize distant eigenstates in

[i] The localization of the eigenstates can also be seen by performing a Jordan-Wigner transformation on the Hamiltonian, which maps to a model of fermion occupation with hopping interactions.

configuration space. Although the small matrix elements may be compensated for by small energy differences between pairs of eigenstates, the occurrence of such "resonances" is rare for sufficiently large disorder. Hence, the weak interaction serves only to "dress" the LIOMs and the system is said to be in the MBL phase[6,8,17]. Meanwhile, in the strong-interaction regime ($J >> W$) the eigenstates become delocalized due to resonant admixing of eigenstates, and the presence of integrability-breaking interactions gives rise to a robustly thermal phase. The competition between the disorder strength and the strength of local interactions generates the transition that separates the thermal and localized phases.

B. Diagnosing Emergent Integrability Using Renormalization Flow

Although MBL is known to survive to all orders in perturbation theory even with power-law interactions[1], it is an open question whether the MBL phase is stable to non-perturbative effects. Incidentally, the most compelling evidence for the survival of the MBL phase relies on the existence of a the most compelling evidence for the survival of the MBL phase relies on the existence of a *local* unitary transformation that recasts MBL Hamiltonian into an integrable form in terms of new effective local degrees of freedom[8,12]. Then, the lack of thermalization in the MBL regime can be attributed to an extensive number of emergent integrals of motion. For instance, one expects that deeply within the localized phase, the Hamiltonian written originally in terms of "p-bits," i.e. Pauli operators $\{\boldsymbol{\sigma}_i\}$, can be rewritten as a *local* Hamiltonian in terms of "ℓ-bits" (localized bits) with pseudospin operators $\{\boldsymbol{\tau}_i\}$[6]

$$H = \sum_i \epsilon_i \tau_i^z + \sum_{i<j} \epsilon_{ij} \tau_i^z \tau_j^z + \sum_{i<j<k} \epsilon_{ijk} \tau_i^z \tau_j^z \tau_k^z + \dots \tag{2}$$

where the τ_i^z operators are quasilocal and the coupling constants $\epsilon_{i_1 i_2 \dots}$ decay exponentially for interactions over a longer range.

$$\epsilon_{i_1 \dots i_k} \sim \exp\left(-\max|i_a - i_b|/\xi\right) \tag{3}$$

with some characteristic length scale ξ.

Note that the rewritten Hamiltonian generates time-evolution that conserves *each* τ_i^z. This suggests that MBL systems may be thought of as a class of integrable systems in which the eigenstates look are product states of the ℓ-bits.[6] In this framework, localized systems with strong disorder are diagonalized by eigenstates which have compact support on the many-body system, with some characteristic localization length[6,7].

Finding a local transformation that diagonalizes the Hamiltonian is challenging. This stems from the fact that there are infinitely many choices for the LIOMs (any linear combination of them is also conserved), and only a restricted set of unitary transformations will result in maximally-localized ℓ-bits. One approach uses the long-time evolved average of the initially local p-bit operators as the LIOMs[3]. The reasoning there was that the time evolution causes the operators to grow more nonlocal but the nonlocal parts are averaged out due to their oscillatory behavior. However, because this method employs exact diagonalization, it is really only accessible for small system sizes. A promising alternative is to define a type of renormalization group flow that performs a succession of local similarity transformations that eventually diagonalizes the Hamiltonian. In this case, the flow encodes a unitary transformation that maps the p-bits to the ℓ-bits. Once the Hamiltonian is diagonalized, one can then evaluate degree of locality from the coupling constants, and also study other properties of the MBL Hamiltonian (entanglement entropy, level statistics, etc).

There are several ways one can go about defining the RG rules for the aforementioned "Hamiltonian-space" flow. In the following sections, we discuss two different methods that have recently been implemented in MBL systems: 1) Wilson-Wegner Flow (WWF)[14,23] and 2) Spectrum Bifurcation RG (SBRG)[16,22]. In WWF, one defines a continuous flow parameter that characterizes the energy scale one is operating at in the RG step. Then, the rules for the flow are governed by a differential equation for the elements of H that reduces the magnitude of the off-diagonal elements. Meanwhile, spectrum bifurcation involves a *discrete* RG flow with a finite total number of steps. At each step, the largest energy scale is identified and block diagonalized with a unitary transformation. This is repeated for the next highest energy scale until the block sizes reduce to 1.

In both the WWF and SBRG, the total unitary transformation implementing the diagonalization may be visualized as a tensor network acting on the matrix product representation of the Hamiltonian. Viewing the RG protocol in this way provides two main advantages: 1) for a large class of MBL Hamiltonians, the RG flow may be implemented entirely using matrix product operators, which can speed up computation 2) the tensor-network picture admits a holographic interpretation, which can give physical insight into the entanglement properties of the MBL system. By relating the network to a physical geometry connecting the boundary p-bits to the bulk ℓ-bits, one can diagnose the localization of the Hamiltonian using geometric features.

II. WILSON-WEGNER FLOW

In this section, we review the Wilson-Wegner Flow (WWF) method implemented in Refs [14,23]. The general WWF protocol, first developed for non-perturbative QCD[21], is a way to continuously flow the Hamiltonian towards its diagonalized form by applying a continuously-varying unitary transformation. In typical real-space RG schemes, one coarse-grains the degrees of freedom to ob-

tain an effective low-energy Hamiltonian. In contrast, the WWF preserves the number of degrees of freedom while decoupling those that are separated by large energy scales. Roughly speaking, one can think of WWF as introducing an energy scale β, and then performing a similarity transformation $H_\beta = U_\beta H U_\beta^\dagger$ so that the "dressed" Hamiltonian H_β describes only processes that correspond to an energy transfer of β or less.[20] The flow towards higher β then moves towards progressively smaller energy scales.

The procedure begins by separating the Hamiltonian into diagonal (H_0) and off-diagonal (V) terms with respect to a physically-motivated basis[14]:

$$H(\beta) = H_0(\beta) + V(\beta) \tag{4}$$

The anti-Hermitian generator of the transforming unitary is defined to be

$$\eta(\beta) = [H_0(\beta), V(\beta)] \tag{5}$$

The differential equations governing the flow are

$$\frac{dU(\beta)}{d\beta} = \eta(\beta) \tag{6}$$

$$\frac{dH(\beta)}{d\beta} = [\eta(\beta), H(\beta)] \tag{7}$$

with initial conditions $U(0) = \mathbb{1}$ and $H(0) = H$. From the above, one observes that the WWF is a nonlinear flow that proceeds more slowly as the Hamiltonian is nearly diagonalized. The total transformation up until scale β is performed by

$$U(\beta) = \mathcal{T}\left\{\exp\left(\int_\beta^\infty d\tau \eta(\tau)\right)\right\} \tag{8}$$

where $\mathcal{T}$ orders the operators by increasing β. The output of the flow are the desired quantities $H(\infty)$ and $U(\infty)$.

To get some intuition for what the WWF does, one can explicitly write out the matrix elements of the generator

$$\eta_{jk} = (\varepsilon_j - \varepsilon_k) V_{jk} \tag{9}$$

where ε_i are the diagonal elements of H_0. We see that the generator weights the matrix elements of the off-diagonal part by the energy separation of the associated states. The evolution of the matrix elements of the Hamiltonian are thus governed by

$$\frac{dH_{jk}}{d\beta} = \sum_m (\varepsilon_j + \varepsilon_k - 2\varepsilon_m) H_{jm} H_{mk} \tag{10}$$

Note that the WWF procedure generically introduces new interaction terms. While this may seem undesirable, this formulation also enables one to integrate past resonances in the diagonal terms that would otherwise complicate perturbative treatments of MBL Hamiltonians[14].

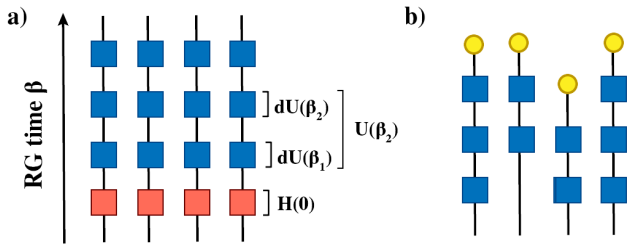

FIG. 1: **a)** A schematic of the matrix product representation of the original Hamiltonian evolving under an infinite stack of infinitesimal unitary transformations. The total unitary transformation $U(\beta)$ is a composition of the infinitesimal $dU(\beta_i)$ implemented at each step. **b)** The final unitary tensor network may be contracted with an ℓ-bit eigenstate matrix product state to yield a tensor-network transformation that acts on the p-bit state. For states which are not rotated at a particular step, the local ℓ-bit index may be brought down to a smaller β, as visualized by lowering the yellow dot. Adapted from [23]

Hence, the power of the WWF RG lies in its non-perturbative capabilities. The final product of the WWF is not a renormalized Hamiltonian but a Hamiltonian that is diagonalized or nearly-diagonalized so that even first approximations capture the physics. Note that the RG "time" parameter is related to the energy scale being addressed in the Hamiltonian as $\beta \propto 1/E^2$.

We shall now discuss how the WWF may be adapted using a tensor network formalism, as done in the study by Yu et. al.[23] The final similarity transformation of the Hamiltonian may be viewed as a chain of unitary operations performed on the eigenstates

$$\langle E|\ldots U(\beta_2)U(\beta_1)HU^\dagger(\beta_1)U^\dagger(\beta_2)\ldots|E\rangle = \tag{11}$$

$$\left\langle (U^\dagger(\beta_1)U^\dagger(\beta_2)E\middle|H\middle|(U^\dagger(\beta_1)U^\dagger(\beta_2)\ldots)E\right\rangle \tag{12}$$

To simulate this efficiently, one can represent the Hamiltonian and unitary transformations using matrix product operators. The matrix product operator (MPO) representation of a matrix is defined as a factorization of the matrix into a product of smaller tensors. This is straightforward to construct for Hamiltonians written in terms of local operators. MPOs are visually denoted by a chain of blocks representing local tensors, connected by bonds that represent the contracted indices (see Fig 1a). Programatically, one can think of a basis of four 2x2 matrices living at each site of the MPO so that performing various operations translates into manipulations of the coefficients of these small matrices. This allows one to avoid working with exponentially large matrices. For instance, extracting the diagonal terms of the Hamiltonian (the first part of a WWF step) corresponds to setting the coefficients of the off-diagonal 2x2 matrices to 0. To actually implement the WWF, one can evolve the flow equations by introducing a small $\Delta\beta$ and expanding $H(\beta+\Delta\beta)$ and $U(\beta+\Delta\beta)$ accordingly. The Hamiltonian

is diagonalized when $\beta(\epsilon_i - \epsilon_j)^2 \sim 1$.

Fig. 1 shows a visual representation of the TWWF procedure. In the work by Yu and colleagues, they investigated the disordered random-field Heisenberg model in Eq. 1 (without any extra interaction terms) with $L = 32$ sites and an initial $J = 1$. A similar WWF procedure was carried out by Pekker et. al[14] with the same Hamiltonian, but without using MPO technology. The findings of the two studies are summarized below:

- **Scale-Invariant Couplings:** The probability distribution of the emergent couplings J normalized by the median value is independent of the physical range of the coupling[14]. For small couplings, the probability distribution evolves smoothly towards a "1/f"-type distribution in the localized phase ($\mathbb{P}(\mathrm{J}) \sim 1/J$) and a uniform distribution in the ergodic phase ($\mathbb{P}(\mathrm{J}) \sim 1$).

- **Operator spreading**: The spread of the horizontal operator size r when transforming the p-bits to the ℓ-bits mimics the logarithmic spread of entanglement in the localized phase $r(\beta) \sim \log(\beta/\beta_0)$ and the Lieb-Robinson bound in the delocalized phase $r(\beta) \sim \beta^{\frac{1}{2}}$. This suggests that information about the entanglement dynamics in different phases is imprinted on the WWF flow dynamics.

- **Energy Scales:** The variance $V(\beta)$, defined to be the average off-diagonal element of $H(\beta)$, can be used to deduce the energy scale being probed at each RG step. Yu et. al. found that the *change* in energy scale is reduced at an exponential rate, but the distribution of the rate is broader for the MBL phase. Furthermore, the minimum energy scale is roughly constant for small disorder, indicating level repulsion (ergodic phase) but increases with the disorder strength in the localized phase, as expected.

- **Emergent Bulk Geometry**: The "size" of the tensor network in TWWF decreases exponentially with vertical distance (defined below) in the localized phase but slows in the ergodic phase.

We will elaborate more on this last point. One of the benefits of the tensor network formalism is that it allows one to generate a geometric picture of how the ℓ-bits emerge from the WWF flow. To define an emergent geometry of the network, one needs to define a measure of vertical distance that captures how far along one is in the diagonalization process with increasing RG time. A natural choice is to use the rate at which the off-diagonal terms of the Hamiltonian decrease

$$D_U(\beta) = \int_0^\beta \sqrt{\frac{\mathrm{Tr}(\eta(\tau)\eta^\dagger(\tau))}{\dim(H)L}} d\tau \tag{13}$$

where $D_U(\beta)$ is the vertical distance of the unitary tensor network up until RG time β, $\mathrm{Tr}\big(\eta(\beta)\eta^\dagger(\beta)\big)$ captures the progression $\eta \to 0$, and $\dim(H)L$ is a rescaling factor present to map $\mathrm{Tr}(\mathbb{1})$ to 1.

One can now examine the evolution of the properties of the tensor network with distance D_U, such as its "size." The measure of bulk size used by Yu, et. al. is the number horizontal tensor bonds that do not have unit bond dimension, which they call the "circumference." The bond dimension is the number of indices contracted between two adjacent tensors in an MPO. A unit bond dimension indicates that a particular unitary chain $dU(\beta)$ has separated into two independent components. This indicates that the adjacent ℓ-bits have been mostly disentangled. One finds that in the localized phase, the circumference decreases exponentially while in the ergodic phase, the coefficient of the exponential decay approaches 0. This can be understood intuitively by recalling the meaning of the flow parameter. The flow parameter characterizes the energy scale that one is disentangling at each RG step. Hence, the exponential decay of the circumference in the MBL phase reflects the scarcity of random "resonances" in the spectrum, while these rare regions proliferate in the ergodic phase. Deep in the MBL phase, one finds a tensor network bulk that is "segmented" with spatially distant points largely disconnected[23].

A comparison of the performance of WWF with other methods like Jacobi rotations for diagonalization or bipartite matching was performed in Ref [14], with the conclusion that the WWF produces the most local unitary. The computational complexity of the TWWF implementation scales polynomially in the bond dimension. Interestingly, both studies of WWF found that the bond dimension deep in the MBL phase is small and bounded. This is likely related to the connection between the reduced spread of entanglement in the localized phase, and the efficiency of simulating the dynamics classically[2]. The idea of MBL systems being accessible to efficient classical simulation reappears in the following survey of a related RG diagonalization procedure.

III. SPECTRUM BIFURCATION RG

The spectrum-bifurcation RG method (SBRG), developed in Ref [22], can be seen as a discrete approximation to the regular WWF flow. Rather than defining a unitary transformation as a function of a continuous parameter, a discrete sequence of block-diagonalizations is executed, with the leading energy scale being targeted at each step. The systematic elimination of the highest energy scales is reminiscent of the aforementioned WWF as well as the hierarchal structure of relevant many-body resonances in recent real-space RG treatments[15,19]. The output of the SBRG procedure is the Hamiltonian written in terms of an approximate set of eigenstates in MPS representation. These eigenstates show the local behavior expected of the new LIOMs in the MBL phase.

There are other methods for producing the MPS rep-

resentations of eigenstates, the most well-known of them being density matrix renormalization group (DMRG). DMRG is designed to produce ground states, though it has been generalized to target highly-excited states as well. The advantage of the SBRG is that it provides a more efficient, albeit less accurate, procedure for finding all eigenstates. The boost in efficiency is derived from the fact that the SBRG relies on Clifford gates, which are known to be computationally economical to implement. Another motivation for the SBRG comes from its holographic interpretation, which gives geometric meaning to the RG flow. In this framework, a Clifford circuit maps the the boundary (physical) degrees of freedom to the bulk (emergent) degrees of freedom which are the conserved LIOMs.

To illustrate the method, we begin with a general set of Hamiltonians of the form

$$H = \sum_{[\mu]} h_{[\mu]} \sigma^{[\mu]} \tag{14}$$

where μ is a multi-index, $\sigma^{[\mu]}$ is a Pauli array of operators, and $h_{[\mu]}$ is the associated coefficient. Any spin or fermion model in an arbitrary number of dimensions can be written in this manner. For instance, the Hamiltonian in Eq. 1 can be written in the above form since both the field terms and interaction terms may be written as a sum of Pauli strings. In that case, $[\mu]$ keeps track of the index of the Pauli operators in the Pauli string. As an example,

$$\begin{aligned} h_i \sigma_i^z &\to h_{300\ldots}(\sigma^3 \otimes \mathbb{1}^{\otimes N-1}) + h_{0300\ldots}(\mathbb{1} \otimes \sigma^3 \otimes \mathbb{1}^{\otimes N-2}) + \cdots \\ J_{ij}^x \sigma_i^x \sigma_j^x &\to h_{110\ldots}(\sigma^1 \otimes \sigma^1 \otimes \mathbb{1}^{\otimes N-2}) \\ &\quad + h_{0110\ldots}(\mathbb{1} \otimes \sigma^1 \otimes \sigma^1 \otimes \mathbb{1}^{\otimes N-3}) + \ldots \end{aligned}$$

Hence, Eq. 14 captures a wide range of possible Hamiltonians including those with multi-qubit and/or nonlocal interactions.

To execute the SBRG, we will:

1. Pick the largest energy scale, which is the largest value of $h_{[\mu]}$ in the Hamiltonian.

2. Block-diagonalize the leading term using Clifford group rotations so that it becomes $H_0 = h_{\max}\sigma^{3[0\ldots]}$. This *bifurcates* the spectrum into high energy $E \simeq |h_{\max}|$ and low energy $E \simeq -|h_{\max}|$ sectors.

3. Classify the remaining terms in the Hamiltonian into the two blocks. This is done by applying a Schrieffer-Wolff transformation thats terms so that all terms in the Hamiltonian commute to at least second-order. Now all terms have been classified into the two blocks.

4. Separate the part of the Hamiltonian that is *not* part of H_0 and repeat the procedure with this part.

Let us now examine the steps in more detail. Block-diagonalization is executed using Clifford group rotations, which rotate Pauli strings into other Pauli strings. A Clifford rotation is applied to the leading energy term in the Hamiltonian is rotated so that

$$\sigma^{[\mu]_{\max}} \to R^\dagger \sigma^{[\mu]_{\max}} R = \sigma^{3[00\ldots]} \tag{15}$$

where $\sigma^{3[00\ldots]}$ represents the tensor product of σ^3 with a series of identity matrices. Note that the appropriate transformation to apply R is operator dependent. Strictly speaking, one need not apply a rotation that places the σ^3 operator at the first qubit; indeed, one can apply a rotation that preserves the locality present in the physical Hamiltonian. However, it is helpful to organize the indices in the order that they are block diagonalized for illustrative purposes.

The Clifford group may be generated by the $\frac{\pi}{4}$ (C_4) phase gate such that

$$R_{C_4}(\sigma^{[\mu]}) \equiv \exp\left(\frac{i\pi}{4}\sigma^{[\mu]}\right) = \frac{1}{\sqrt{2}}(1 + i\sigma^{[\mu]}) \tag{16}$$

It can be shown that its adjoint action yields

$$R_{C_4}^\dagger(\sigma^{[\mu]})\sigma^{[\nu]}R_{C_4}(\sigma^{[\mu]}) = \begin{cases} \sigma^{[\nu]} & \text{if } \sigma^{[\mu]}, \sigma^{[\nu]} \text{ commute} \\ i\sigma^{[\nu]}\sigma^{[\mu]} & \text{if } \sigma^{[\mu]}, \sigma^{[\nu]} \text{ anticommute} \end{cases} \tag{17}$$

Using this, one can transform any Pauli string into any other Pauli string. As an example, consider a term of the form $\sigma^{[\lambda][\mu]}$ where the first set of indices $\lambda \in \{0, 3\}$ and the latter indices $\mu \in \{0, 1, 2, 3\}$). Suppose that the first μ index is $\mu = 1$. Then one can diagonalize the term by applying a transformation as follows:

$$\sigma^{[\lambda]1[\mu]} \xrightarrow{R_{C_4}(i\sigma^{[\lambda]2[\mu]})} \sigma^{[0\ldots]3[0\ldots]} \tag{18}$$

Then, swap operations may be applied to bring σ^3 to any position within the string. Hence, we have a set of operations sufficient to perform our successive block diagonalizations.

Consider the form of the Hamiltonian after the first block-diagonalization. A transformation R is applied to the entire Hamiltonian so that $H \to H' = R^\dagger H R$ and the leading energy term becomes $H_0 = h_{\max}\sigma^{3[\mu]}$. The Hamiltonian can then be split up into terms that commute with H_0 and terms that anti-commute with H_0.

$$H = H_0 + \Delta + \Sigma \tag{19}$$

where Δ represents the commuting terms of the form $\sigma^{\lambda[\nu]}$ with $\lambda \in \{0, 3\}$, $\nu \in \{0, 1, 2, 3\}$ and Σ represent the anti-commuting terms of the same form where $\lambda \in \{1, 2\}$. Notice that all terms in H *must* fall into the two classes Δ and Σ. Since Δ contains commuting terms, it lives within the diagonal blocks. So one needs only to sort the terms of Σ into one of the two blocks $|h_{\max}|$ and

$-|h_{\max}|$. This may be done by applying a Schrieffer-Wolff transformation,

$$S = \exp\left(-\frac{1}{2h_{\max}^2} H_0 \Sigma\right) \tag{20}$$

Expanding S to second order in $h_{\max}$ and applying the similarity transformation yields

$$H = H_0 + \Delta - \frac{1}{2h_{\max}^2} \Sigma^{-1} H_0 \Sigma \tag{21}$$

$$= H_0 + \Delta + \frac{1}{2h_{\max}^2} H_0 \Sigma^2 \tag{22}$$

All of the above terms commute and therefore we have block diagonalized the Hamiltonian to second order. Note that the second order approximation is justified for sufficiently large $h_{\max}$, which is good approximation for an MBL system with strong disorder (and hence, large separation in energy scales). Hence, the SBRG provides an efficient method of finding eigenstates deep in the localized phase, but begins to fail near the transition to the delocalization.

Grouping the terms $\Delta + \frac{1}{2h_{\max}^2} H_0 \Sigma^2$, one has

$$H = h_{\max} \sigma^{3[0\ldots]} + \sum_{[\mu]} h_{\lambda[\mu]} \sigma^{\lambda[\mu]} \tag{23}$$

The first term is identified as an emergent quantity while the second term is subsequently block-diagonalized with finer granularity in the next SBRG step. The reason we can identify $\sigma^{3[0\ldots]}$ as an emergent LIOM is because its energy scale is much higher than its local neighbors, so it is unlikely to be flipped as one moves towards lower frequencies. Hence, it remains untouched by the rest of the SBRG procedure. Because the SBRG allows new terms to be generated, it allows one to overcome limitations associated with conventional closed-form RG. The final result is a diagonal Hamiltonian of the form

$$H = \sum_{[\lambda=0,3]} h_{[\lambda]} \sigma^{[\lambda]} \tag{24}$$

from which one can immediately read off the spectrum from $h_{[\mu]}$.

A visualization of the SBRG procedure is shown in Fig. 2a, as well as a example of an RG step for the disordered quantum Ising chain, given by the Hamiltonian

$$H = -\sum_i J_i \sigma_i^1 \sigma_{i+1}^1 + K_i \sigma_i^3 \sigma_{i+1}^3 + h_i \sigma_i^3 \tag{25}$$

with K_i, J_i, h_i as random independent variables drawn from identical distributions of the form

$$P(v)dv = \frac{1}{\Gamma_0 v} \left(\frac{v}{v_0}\right)^{1/\Gamma_0} dv \text{ for } v \in [0, v_0] \tag{26}$$

where v is a placeholder for the relevant random coupling constant. Γ_0 sets the global disorder strength whereas v_0 sets the individual coupling strength.

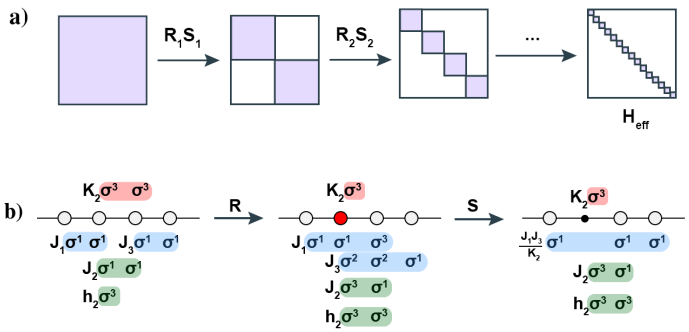

FIG. 2: **a)** Schematic of the iterative block-diagonal procedure of SBRG from higher to lower energy scales. **b)** Visual outline of the basic SBRG procedure applied to the disordered quantum Ising model. The Pauli string associated to the leading energy term is represented in red, whereas the commuting terms Δ are in blue and the anti-commuting terms Σ are in green. H_0 is diagonalized by R, and the emergent qubit is shown as a red dot. The block off-diagonal terms associated with J_1 and J_2 are treated perturbatively and a Schrieffer-Wolff transformation S yields the effective couplings. H_0 is left untouched by S. Adapted from [22].

The final output of SBRG procedure are product eigenstates in the emergent ℓ-bit basis, $|\{\tau_i\}\rangle = |\tau_1\rangle \otimes |\tau_2\rangle \otimes \ldots$. To obtain the eigenstates in terms of the original basis, one needs to reverse the unitary transformation applied by the SBRG, $|\psi_{\{\tau_i\}}\rangle \simeq U_{RG} |\{\tau_i\}\rangle$ where

$$U_{RG} = \prod_k R_k S_k \tag{27}$$

is the total unitary transformation performed in the flow.

To get a sense of the performance of the SBRG in identifying the emergent LIOMs, one can analyze *how* local the Hamiltonian is. This can be done by examining the decay of the coupling constants in the interaction terms in Eq. 2.

Like the TWWF RG procedure, SBRG also admits a holographic interpretation since it is mediated by a series of Hilbert space-preserving unitary transformations. It turns out the predominant contributions to U_{RG} come from the Clifford gates (with negligible rotations from the Schrieffer-Wolff transformations), and so the entire flow can be approximated as a random Clifford circuit[22]. Unsurprisingly, the locality of the Clifford operators reflects the degree of localization in the Hamiltonian. The Clifford stabilizers[ii] are primarily concentrated in the UV (high energy) regime, reflecting the ability of the SBRG to disentangle the bulk qubits efficiently. Longer stabilizers that span more physical qubits are rare, and only appear in the IR (low energy) regime in systems near

[ii] They are stabilizers in the sense that every eigenstate in the physical Hilbert space is stabilized by $\hat{\tau}_i$ to ± 1 such that $\hat{\tau}_i |\psi_{\tau_i}\rangle = \pm |\psi_{\tau_i}\rangle$

MBL criticality. For instance, when $K_0 = 0$ and $J_0 = h_0$, one is at the marginal MBL critical point of the transverse field Ising model, and consequently, observes the spread of the stabilizers. Interestingly, at late RG time, the procedure yields a long stabilizer string which corresponds to the Jordan-Wigner transformation that maps the TFIM to free Majoranas! Performing a more quantitative study of the localization length of the stabilizers reveals that the probability distributions of the lengths decrease. Specifically, deeply *within* an MBL phase, the probability decreases exponentially while closer to the marginal MBL critical point, the probability decreases like a power law.

Let us now examine the holographic geometry that arises from the SBRG of an MBL system from a more intuitive perspective. In our holographic model, we will plant the physical degrees of freedom on the boundary of some circular geometry and the emergent degrees of freedom within the bulk interior. For the disordered MBL system, the RG flow is approximately mediated by Clifford gates, each of which identifies an emergent qubit. The energy scale of the emergent qubit is characterized by the Clifford gate's depth within the bulk of the circuit, which one associates to a radial position in the bulk. Then the Clifford circuit manifests as a disentangler network mapping the boundary eigenstates (IR) to an emergent bulk product state (UV). The transformations in the network depend on the state selected on all of the emergent UV qubits. This is because the selected state locates the system at a certain energy density in the spectrum, affecting the IR transformations, and this UV-IR mixing is encoded in the many-body terms of the ℓ-bit Hamiltonian. The result is a geometry that appears largely fragmented, with nearby boundary degrees of freedom becoming mixed by transformations but far-separated qubits remaining disconnected. A visual representation of this is shown in Fig. 3. Note that this characterization of the geometry is analogous to the fragmented geometry found in the TWWF study.

IV. CONCLUSION

In summary, we have discussed two new recent implementations of Hamiltonian-space RG for studying MBL systems. These RG protocols are designed to recast the MBL Hamiltonian in terms of its emergent LIOMs, providing stronger evidence of the emergent integrability of MBL systems. Both methods generate the RG flow through a succession of unitary transformations that progressively eliminate large energy scales, which may be understood as creating a hierarchy of relevant interactions based on the many-body level spacing. Furthermore, the RG methods are compatible with large systems sizes—a feature useful to the study of the MBL phase in the thermodynamic limit. The first method discussed (TWWF) takes advantage of tensor network technology to perform the unitary transformations efficiently, while the second method (SBRG) offers a further boost in efficiency by performing a discretized, bounded flow at the cost of accuracy, which decreases in the strong disorder limit. A unique feature of these Hilbert space-preserving RGs is that the flow may be understood as being mediated by a holographic tensor network. This interpretation allows one to understand the mapping between the p-bits and emergent ℓ-bits geometrically. The studies discussed found that the entanglement properties in the MBL phase leave an imprint on the structure of the tensor network bulk. An important observation is the connection between the "area-law" entanglement present in the MBL phase, the fragmentation of the bulk geometry, and the computational efficiency associated with classical simulation of the RG flow. By borrowing intuition from holographic duality, one could potentially better understand MBL systems and the many-body localized transition.

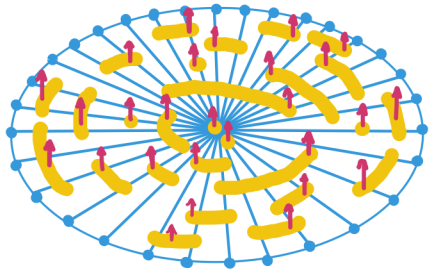

FIG. 3: Fragmented holographic geometry of an MBL system under the SBRG. Yellow blocks represent the Clifford gates, blue dots the physical qubits, and red arrows the emergent qubits. Adapted from [22].

[1] Denis M Basko, Igor L Aleiner, and Boris L Altshuler. Metal–insulator transition in a weakly interacting many-electron system with localized single-particle states. *Annals of physics*, 321(5):1126–1205, 2006.

[2] Bela Bauer and Chetan Nayak. Area laws in a many-body localized state and its implications for topological order. *Journal of Statistical Mechanics: Theory and Experiment*, 2013(09):P09005, 2013.

[3] Anushya Chandran, Isaac H Kim, Guifre Vidal, and Dmitry A Abanin. Constructing local integrals of motion in the many-body localized phase. *Physical Review B*, 91(8):085425, 2015.

[4] Joshua M Deutsch. Eigenstate thermalization hypothesis. *Reports on Progress in Physics*, 81(8):082001, 2018.

[5] Philipp T Dumitrescu, Anna Goremykina, Siddharth A Parameswaran, Maksym Serbyn, and Romain Vasseur.

Kosterlitz-thouless scaling at many-body localization phase transitions. *Physical Review B*, 99(9):094205, 2019.

[6] David A Huse, Rahul Nandkishore, and Vadim Oganesyan. Phenomenology of fully many-body-localized systems. *Physical Review B*, 90(17):174202, 2014.

[7] David A Huse, Rahul Nandkishore, Vadim Oganesyan, Arijeet Pal, and Shivaji L Sondhi. Localization-protected quantum order. *Physical Review B*, 88(1):014206, 2013.

[8] John Z Imbrie. On many-body localization for quantum spin chains. *Journal of Statistical Physics*, 163(5):998–1048, 2016.

[9] Vedika Khemani, Say-Peng Lim, DN Sheng, and David A Huse. Critical properties of the many-body localization transition. *Physical Review X*, 7(2):021013, 2017.

[10] David J Luitz, Nicolas Laflorencie, and Fabien Alet. Many-body localization edge in the random-field heisenberg chain. *Physical Review B*, 91(8):081103, 2015.

[11] Rahul Nandkishore and David A Huse. Many-body localization and thermalization in quantum statistical mechanics. *Annu. Rev. Condens. Matter Phys.*, 6(1):15–38, 2015.

[12] Arun Nanduri, Hyungwon Kim, and David A Huse. Entanglement spreading in a many-body localized system. *Physical Review B*, 90(6):064201, 2014.

[13] Arijeet Pal and David A Huse. Many-body localization phase transition. *Physical Review B*, 82(17):174411, 2010.

[14] David Pekker, Bryan K Clark, Vadim Oganesyan, and Gil Refael. Fixed points of wegner-wilson flows and many-body localization. *Physical review letters*, 119(7):075701, 2017.

[15] Andrew C Potter, Romain Vasseur, and SA Parameswaran. Universal properties of many-body delocalization transitions. *Physical Review X*, 5(3):031033, 2015.

[16] Louk Rademaker and Miguel Ortuno. Explicit local integrals of motion for the many-body localized state. *Physical review letters*, 116(1):010404, 2016.

[17] Valentina Ros, Markus Müller, and Antonello Scardicchio. Integrals of motion in the many-body localized phase. *Nuclear Physics B*, 891:420–465, 2015.

[18] Mark Srednicki. Chaos and quantum thermalization. *Physical Review E*, 50(2):888, 1994.

[19] Ronen Vosk, David A Huse, and Ehud Altman. Theory of the many-body localization transition in one-dimensional systems. *Physical Review X*, 5(3):031032, 2015.

[20] TS Walhout. Similarity renormalization, hamiltonian flow equations, and dyson's intermediate representation. *Physical Review D*, 59(6):065009, 1999.

[21] Kenneth G Wilson, Timothy S Walhout, Avaroth Harindranath, Wei-Min Zhang, Robert J Perry, and Stanisław D Głazek. Nonperturbative qcd: A weak-coupling treatment on the light front. *Physical Review D*, 49(12):6720, 1994.

[22] Yi-Zhuang You, Xiao-Liang Qi, and Cenke Xu. Entanglement holographic mapping of many-body localized system by spectrum bifurcation renormalization group. *Physical Review B*, 93(10):104205, 2016.

[23] Xiongjie Yu, David Pekker, and Bryan K Clark. Bulk geometry of the many body localized phase from wilson-wegner flow. *arXiv preprint arXiv:1909.11097*, 2019.